

Accelerated Publications

Photocycle of the Flavin-Binding Photoreceptor AppA, a Bacterial Transcriptional Antirepressor of Photosynthesis Genes[†]

Magdalena Gauden,^{‡,§} Sergey Yermenko,^{§,||} Wouter Laan,^{||} Ivo H. M. van Stokkum,[‡] Janne A. Ihalainen,[‡] Rienk van Grondelle,[‡] Klaas J. Hellingwerf,^{*,||} and John T. M. Kennis^{*,‡}

Department of Biophysics, Faculty of Sciences, Vrije Universiteit, De Boelelaan 1081, 1081 HV Amsterdam, The Netherlands, and Swammerdam Institute for Life Sciences, University of Amsterdam, Nieuwe Achtergracht 166, 1018 WY Amsterdam, The Netherlands

Received December 16, 2004; Revised Manuscript Received January 26, 2005

ABSTRACT: The flavoprotein AppA from *Rhodobacter sphaeroides* contains an N-terminal domain belonging to a new class of photoreceptors designated BLUF domains. AppA was shown to control photosynthesis gene expression in response to blue light and oxygen tension. We have investigated the photocycle of the AppA BLUF domain by ultrafast fluorescence, femtosecond transient absorption, and nanosecond flash-photolysis spectroscopy. Time-resolved fluorescence experiments revealed four components of flavin adenine dinucleotide (FAD) excited-state decay, with lifetimes of 25 ps, 150 ps, 670 ps, and 3.8 ns. Ultrafast transient absorption spectroscopy revealed rapid internal conversion and vibrational cooling processes on excited FAD with time constants of 250 fs and 1.2 ps, and a multiexponential decay with effective time constants of 90 ps, 590 ps, and 2.7 ns. Concomitant with the decay of excited FAD, the rise of a species with a narrow absorption difference band near 495 nm was detected which spectrally resembles the long-living signaling state of AppA. Consistent with these results, the nanosecond flash-photolysis measurements indicated that formation of the signaling state was complete within the time resolution of 10 ns. No further changes were detected up to 15 μ s. The quantum yield of the signaling-state formation was determined to be 24%. Thus, the signaling state of the AppA BLUF domain is formed on the ultrafast time scale directly from the FAD singlet excited state, without any apparent intermediate, and remains stable over 12 decades of time. In parallel with the signaling state, the FAD triplet state is formed from the FAD singlet excited state at 9% efficiency as a side reaction of the AppA photocycle.

Photosynthetic organisms are able to respond to a wide range of signals from the environment; one of the most

important of these is light. Plants, algae, and photosynthetic bacteria have developed elaborate systems for signal perception and transduction of UV, visible, and near-IR radiation, for growing, developing, and adjusting optimally to the ambient light climate (1–4). Most of these light sensors can be classified in one of six major families of photosensor proteins. In three of these, the rhodopsins, the xanthopsins, and the phytochromes, their activation is based on light-induced *E/Z* isomerization (1). The other three families (cryptochromes, phototropins, and BLUF¹ domains) all contain a flavin as their light-absorbing entity. However, except for the LOV domains of phototropins, in which a

[†]M.G., S.Y., and W.L. were supported by the Netherlands Organization for Scientific Research through the Chemical Sciences Council (NWO-CW). The work of J.A.I. is supported by European Community's Human Potential Program Grant HPRN-CT-2002-00248 (PSICO). J.T.M.K. was supported by the Life Sciences Council of the Netherlands Organization for Scientific Research (NWO-ALW) via a VIDI fellowship.

* To whom correspondence should be addressed. E-mail: khelling@science.uva.nl or j.kennis@few.vu.nl.

[‡]Vrije Universiteit.

[§]These authors contributed equally.

^{||}University of Amsterdam.

covalent flavin–cysteine adduct is formed upon illumination (5), their primary photochemistry is poorly understood.

The N-terminal domain of the flavoprotein AppA from *Rhodobacter sphaeroides* belongs to the new class of photoreceptors containing a BLUF domain (sensors of blue light using FAD/flavin) (6). AppA was shown to control photosynthesis gene expression in response to high-intensity blue light irradiation. For this function, the N-terminal flavin-binding domain is required. In addition, via its C-terminal domain, AppA can transduce signals generated by variation of the oxygen tension (4, 7, 8). In *R. sphaeroides*, the photosynthetic apparatus is produced at low oxygen tension and low light intensity, whereas under aerobic and high-light conditions, formation of photosynthetic complexes is inhibited by the transcriptional repressor PpsR. Under conditions of low oxygen tension and low light intensity, PpsR is complexed with AppA, which allows transcription to proceed. Blue light disrupts the binding of AppA to PpsR and thereby its anti-repression function, thus restoring the PpsR binding activity to the promoter region of photosynthesis genes such as the *pu*c operon (4).

For several reasons, it is important to further characterize the molecular basis of the photoreceptor function of AppA. (i) Because all the components of this blue light signaling cascade are known (i.e., the receptor AppA, its interaction partner PpsR, and the biological output function, i.e., expression of the photosynthetic machinery), one is able to study biological signal transduction of a light signaling pathway all the way from the initial photon absorption to gene expression, i.e., in a “systems biology” or “synthetic biology” approach. (ii) The predicted secondary structure of the flavin binding BLUF domain of AppA shows no similarity to any of the known flavin binding proteins. This domain has therefore been proposed to represent a novel flavin binding fold, and it remains to be resolved experimentally how its (flavin-based) photochemistry proceeds (6).

So far, it has been shown that blue light excitation of AppA induces a photocycle in which a long-lived signaling state is formed which shows an ~ 10 nm red-shifted absorption spectrum. The formation of the signaling state is associated with conformational changes in the protein (8–10) that then result in the inability of AppA to form a stable AppA–PpsR complex. The red shift was originally proposed to result from altered π – π stacking interaction between a tyrosine, conserved in all BLUF sequences known to date, and the flavin isoalloxazine ring, along with a hydrogen bond rearrangement between N5 of the flavin ring and the tyrosine (9). The FAD cofactor may also be deprotonated in the signaling state (10). FTIR spectroscopy on another BLUF domain, the *slr1694* protein from *Synechocystis*, showed that light absorption causes a hydrogen bond rearrangement so that the carbonyls of the isoalloxazine ring become more strongly hydrogen-bonded with residues lining the flavin binding pocket. Moreover, a conformational rearrangement of the protein was detected. It is relevant to know, however, that this cyanobacterial BLUF domain exhibits a recovery rate increased 200-fold compared to that of AppA (11).

Little is known of the photochemical events that lead to formation of the red-shifted signaling state. Microsecond flash-photolysis experiments have shown that the signaling state is formed in less than 1 μ s; it was not clear from those data whether intermediates with a nano- or microsecond lifetime preceded the formation of the signaling state (9). Here, we present a comprehensive time-resolved study from the femtosecond to microsecond time scales to determine the reaction rates at which, and intermediate states through which, the photochemistry of the AppA BLUF domain proceeds. Moreover, we have determined the quantum yield of signaling-state formation of this newly discovered photoreceptor protein.

MATERIALS AND METHODS

Protein Expression and Purification. The BLUF domain of AppA, AppA_{5–125}, was cloned, expressed, and nickel affinity purified essentially as described previously (10). However, we recently found that our construct, when expressed in and purified from *Escherichia coli*, binds a mixture of flavins. To produce a homogeneous sample with respect to the chromophore composition, the cell-free extracts were first incubated with a large molar excess of FAD for 1 h on ice before proceeding with the nickel affinity chromatography (see also ref 12). Nickel affinity purified protein was dialyzed overnight against 10 mM Tris-HCl (pH 8.0) and further purified by anion-exchange chromatography on a ResourceQ (6 mL) column (Amersham Biosciences). The proteins were eluted using a gradient of 0 to 1 M NaCl in 10 mM Tris-HCl (pH 8.0) and detected at 280 nm. Eluted proteins with similar UV–vis absorption spectra were pooled and dialyzed to 10 mM Tris-HCl (pH 8.0) and stored at 253 K. The purity of the samples was checked with SDS–PAGE using the PHAST system (Amersham Biosciences) and by UV–vis spectroscopy. The flavin composition of the samples was checked by TLC (12).

Time-Resolved Spectroscopy. Time-resolved fluorescence experiments were performed with a synchroscan streak camera setup described previously (13). The time-resolved fluorescence kinetics were recorded upon excitation at 400 nm at a power of 500 μ W. Pulses with a duration of 100 fs were generated with a 50 kHz repetition rate using an amplified Ti:sapphire laser system (Vitesse-Rega, Coherent Inc., Mountain View, CA). Fluorescence was collected with a right-angle detection geometry using achromatic lenses and detected through a sheet polarizer set at the magic angle (54.7°) with a Hamamatsu C5680 synchroscan camera and a Chromex 250IS spectrograph. The streak images were recorded with a cooled (–55 °C) Hamamatsu C4880 CCD camera. Streak camera images were obtained on a time basis of 500 ps and 2 ns.

Femtosecond transient absorption spectroscopy was carried out with a 1 kHz Ti:sapphire-based regenerative amplification system described previously (14); 400 nm light was obtained by frequency doubling the output of the Ti:sapphire laser, attenuated to 1 μ J, and used as a pump. A white light continuum, generated by focusing the rest of the amplified 800 nm light on a 1 mm CaF₂ crystal, was used as a probe. The probe pulse was focused and overlapped with the excitation beam at the sample position. After passing through

¹ Abbreviations: DAS, decay-associated spectrum; EADS, evolutionary-associated difference spectrum; SADS, species-associated difference spectrum; DADS, decay-associated difference spectrum; FAD, flavin adenine dinucleotide; BLUF, blue light-sensing using FAD/flavin.

the sample, the probe beam was dispersed by a polychromator and projected on a diode array detector. Femtosecond time delays between the pump and probe were controlled by a delay line covering delays up to 4.5 ns. The relative polarization plane of the pump and probe beams was set to the magic angle (54.7°).

The samples were loaded in a flow system with a volume of 10 mL, including a flow cuvette with a path length of 1 mm, and passed by a peristaltic pump. For the time-resolved fluorescence experiment, the absorbance of the sample was adjusted to 0.07 mm⁻¹ at 446 nm, whereas for the femtosecond time-resolved absorption experiment, the absorbance of the sample was adjusted to 0.3 mm⁻¹. The absorption spectrum of the sample was checked during the measurements to verify that the sample remained in the “dark” state.

Nanosecond-to-millisecond transient absorption spectroscopy was carried out using a flash-photolysis spectrometer (Edinburgh Scientific, LP900) equipped with a Q-switched Nd:YAG laser (Continuum Surelight) and an OPO as an excitation source and a Xe-flash lamp for probing. The excitation pulse duration was ~6 ns. Time-gated difference spectra were collected using a CCD detector array equipped with an image intensifier. The time resolution of the apparatus, determined by the detector response time, was ~10 ns. Single-wavelength spectral kinetics were measured by means of a photomultiplier and an oscilloscope (Tektronix TDS 340A). The temporal response of the photomultiplier was <10 ns; however, the signals were slightly distorted during the first microsecond as a result of interference by the Q-switch from the Nd:YAG laser. The optical path length of the sample was 1 cm. Because AppA₅₋₁₂₅ has a dark-state recovery rate on the order of 0.001 s⁻¹, a fresh portion of the solution was provided for each laser flash, allowing a faster averaging of the data. All measurements were performed at 20 °C.

Data Analysis. The time-resolved fluorescence data recorded on time bases of 500 ps and 2 ns were simultaneously globally analyzed in terms of a sum of exponentials to obtain decay-associated spectra (DAS). The femtosecond transient absorption data were globally analyzed using a kinetic model consisting of sequentially interconverting evolution-associated difference spectra (EADS), i.e., 1 → 2 → 3 → ..., in which the arrows indicate successive monoexponential decays of increasing time constants, which can be regarded as the lifetime of each EADS. The first EADS corresponds to the time zero difference spectrum. This procedure enables us to visualize clearly the evolution of the (excited) states of the system. In general, the EADS may well reflect mixtures of molecular states. To further unravel the pathways for product-state formation following light absorption in AppA₅₋₁₂₅, a target analysis was performed in which a specific kinetic scheme was tested. With this procedure, the species-associated difference spectra (SADS) of pure molecular states are estimated. The instrument response function was fit to a Gaussian with a full width at half-maximum of 120 fs for the ultrafast transient absorption experiments, and values of 6 and 13 ps for the time-resolved fluorescence measurements when conducted on the 500 ps and 2 ns time bases, respectively. The global analysis procedures described in this paper have been extensively reviewed in ref 15.

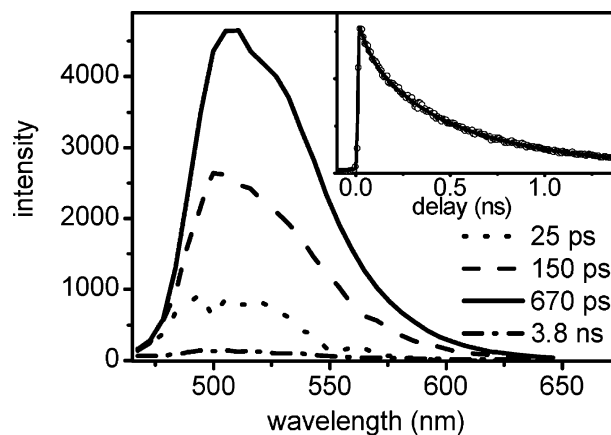


FIGURE 1: Decay-associated spectra (DAS) and associated time constants that follow from a global analysis of the streak camera images obtained from AppA₅₋₁₂₅ upon 400 nm excitation. The inset shows a kinetic trace at 505 nm (○) and the result of the global analysis procedure (—).

RESULTS

Time-Resolved Fluorescence Spectroscopy. The absorption spectrum of AppA₅₋₁₂₅ shows absorption bands at 380 and 446 nm (8), which are assigned to electronic transitions from the ground state to the S₂ and S₁ states of FAD, respectively. We have performed synchroscan streak camera fluorescence experiments on AppA₅₋₁₂₅ to examine its excited-state dynamics. The excitation wavelength was 400 nm, which implies that a mixture of S₁ and S₂ singlet states of FAD was excited. The fluorescence was monitored in a spectral window from 460 to 650 nm. Two time ranges were examined, of 500 ps and 2 ns. A kinetic trace (circles) measured at the maximum of the fluorescence emission band (505 nm) on a 2 ns time basis is depicted in the inset of Figure 1. A global analysis procedure, applied simultaneously on the streak camera data of the two time ranges, yielded four decay components with lifetimes of 25 ps, 150 ps, 670 ps, and 3.8 ns. The solid line in the inset of Figure 1 shows the fitted curve. The decay-associated spectra (DAS) of each component had a maximum around 505 nm and a shoulder around 530 nm. The 670 ps component was dominant with a relative decay amplitude of 0.56, with smaller contributions made by the 25 ps component (amplitude of 0.10) and the 150 ps component (amplitude of 0.32). The longest decay component of 3.8 ns had a very small amplitude of 0.02. This component peaks at the same wavelength as the other components (505 nm), which indicates that it follows from protein-bound FAD and not from free FAD, which peaks near 530 nm (16). The actual streak camera image recorded on the 2 ns time basis is presented in Figure S1 of the Supporting Information to enable a direct comparison with the global analysis results.

Femto- to Nanosecond Transient Absorption Spectroscopy. Femtosecond time-resolved absorption spectroscopy was performed on AppA₅₋₁₂₅ to assess the primary intermediates that ultimately lead to formation of the long-lived signaling state. The sample was excited at 400 nm, and the time-resolved absorbance changes were monitored over a wavelength range from 430 to 675 nm. Figure 2A shows a kinetic trace recorded at 548 nm, which corresponds to a spectral region where stimulated emission from the FAD chromophore is monitored. The stimulated emission signal rises

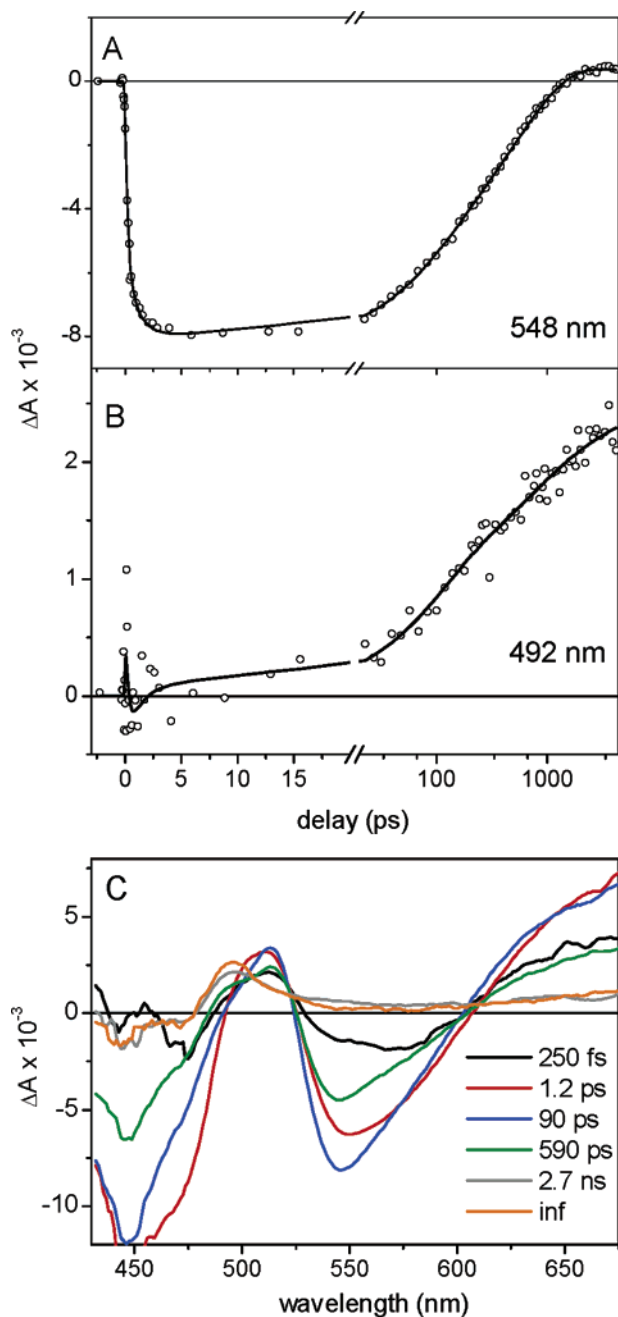


FIGURE 2: (A) Kinetic traces of AppA₁₋₁₂₅ detected at 548 nm (○) upon excitation at 400 nm, along with the result of the global analysis (—). Note that the time axis is linear from -3 to 20 ps, and logarithmic thereafter. (B) Same as panel A with detection at 492 nm. (C) Evolution-associated difference spectra (EADS) and their corresponding lifetimes resulting from global analysis of ultrafast transient absorption experiments on AppA₅₋₁₂₅ upon excitation at 400 nm.

on a time scale of hundreds of femtoseconds to a picosecond, after which we observe a multiexponential decay of the stimulated emission signal on time scales that correspond closely to those obtained with the streak camera in the fluorescence measurements. To visualize the spectral evolution of the system, and enable the identification of transient molecular species in a qualitative way, the time-resolved data were globally analyzed in terms of a kinetic scheme with sequentially interconverting species. Each species is characterized by an evolution-associated difference spectrum (EADS). The global analysis procedure indicated that six

components were required for an adequate description of the time-resolved data, with lifetimes of 250 fs, 1.2 ps, 90 ps, 590 ps, and 2.7 ns and a component that did not decay on the time scale of our experiment. Besides the 250 fs and 1.2 ps components, which could not be resolved in the streak camera experiment because of insufficient time resolution, the transient absorption experiments resolved one FAD decay component less than the streak camera experiment. Thus, the 90 ps, 590 ps, and 2.7 ns components should be regarded as “effective” time constants for a probably more complex multiexponential behavior. Raw time-resolved absorbance difference spectra at selected delays are shown in Figure S2 of the Supporting Information to enable a direct comparison with the results from the global analysis procedure.

The EADS that result from the sequential analysis are presented in Figure 2C, while the solid lines in panels A and B of Figure 2 denote the fits to the kinetic traces. The EADS with a lifetime of 250 fs (black curve) can be assigned to the mixture of initially created singlet excited states of S_1 and S_2 of the FAD chromophore. It shows an overall low amplitude with a ground-state bleach near 450 nm and a stimulated emission band near 550 nm. This EADS evolves in 250 fs to the next EADS, which has a lifetime of 1.2 ps (red line). The stimulated emission band has increased in magnitude, which is due to internal conversion from the S_2 state to the S_1 state. Moreover, a significant increase in the magnitude of the bleach at 450 – 475 nm occurs, which is presumably the result of a loss of excited-state absorption from S_2 in that region. The evolution to the next EADS, which is formed in 1.2 ps and possesses a lifetime of 90 ps, corresponds to an increase and blue shift of the stimulated emission signal near 540 nm, and a loss of ground-state bleach near 450 nm. It is not entirely clear what process underlies this spectral evolution. However, this component was absent upon excitation of AppA₅₋₁₂₅ at 475 nm (not shown), which suggests that it is related to dissipation of the excess energy provided by short-wave excitation at 400 nm. We thus attribute the spectral characteristics of this process to vibrational cooling of the FAD S_1 state. The 90 ps component (blue line) shows a ground-state bleach at 450 – 475 nm, an excited-state absorption at 520 nm, a pronounced stimulated emission around 540 nm, and excited-state absorption at wavelengths longer than 600 nm. This component is assigned to the relaxed FAD S_1 singlet excited state, and exhibits spectral characteristics similar to those of the FMN singlet excited state in the LOV2 domain of phototropin (17). The next EADS, which has a lifetime of 590 ps (green line), exhibits similar features but an overall amplitude smaller than that of the 90 ps component, signaling decay of the FAD singlet excited state. In the fourth EADS, which is formed in 590 ps and decays in 2.7 ns (gray line), the ground-state bleach and stimulated emission bands have largely disappeared. Interestingly, a narrow absorption feature near 497 nm has appeared. This feature resembles that of the difference spectrum of the long-lived AppA signaling state, which peaks at 495 nm (8). Moreover, a weak, broad absorption band is observed in the spectral region between ~ 550 and 675 nm. The evolution that follows from the fifth to the final, nondecaying EADS in 2.7 ns shows a slight increase in the magnitude of the 497 nm absorption band, whereas the rest of the spectrum remains essentially the same.

It thus appears that a photocycle intermediate, which has a narrow absorption feature that spectrally resembles that of the long-lived signaling state, is formed on the sub-nanosecond time scale. This is illustrated clearly in the kinetic trace at 492 nm (Figure 2B), where the photoproduct absorbs almost maximally and the difference spectrum of the relaxed FAD singlet excited state shows an isosbestic point. The signal starts near zero, and increases to a maximum value in the course of hundreds of picoseconds to a few nanoseconds. Close inspection of the 590 ps EADS (Figure 2C, green line) reveals a shoulder near 495 nm which is absent in the 90 ps EADS (blue line). This suggests that formation of the product state near 495 nm takes place in parallel with FAD excited-state decay, i.e., with time constants of 90 and 590 ps. An additional species with a broad absorption in the red (~ 650 nm) is formed as well. On the basis of previous studies on flavins, the positive signal of the nondecaying component at wavelengths longer than 600 nm can be assigned to the triplet state of the protein-bound FAD chromophore (17, 18). This interpretation will be further substantiated by nanosecond flash-photolysis spectroscopy (see below).

Nanosecond Flash-Photolysis Spectroscopy. To further characterize the photocycle of AppA₅₋₁₂₅ and link the ultrafast spectroscopic experiments with those obtained with microsecond-to-second time-resolved spectroscopy (9, 10), we performed transient absorption measurements using a flash-photolysis apparatus that provides a time resolution on the order of 10 ns, with the longest detectable time scale exceeding the microsecond regime. Accordingly, only a minimal time gap remains between the femtosecond-to-nanosecond and nanosecond-to-microsecond transient absorption data. Samples were excited at 450 nm, and time-resolved absorbance changes were monitored in the wavelength range from 400 to 675 nm.

The absorption difference spectra detected 10 ns (solid line), 2 μ s (dotted line), and 15 μ s (dashed line) after the excitation are shown in Figure 3A, along with the nondecaying EADS from the ultrafast data (symbols), reproduced from Figure 2C. The 10 ns absorption difference spectrum is very similar to the nondecaying EADS derived from the ultrafast experiments, with a narrow absorption peak near 498 nm that resembles the long-lived signaling state, and a broad absorption around 650 nm. The 1 nm difference in the peak positions falls within the wavelength calibration accuracies of ± 1.5 nm of the two spectrophotometers. The absorption difference spectrum at 15 μ s perfectly resembles the steady-state difference spectrum of the AppA₅₋₁₂₅ signaling state, with an induced absorption at 495 nm and a bleach at 442 nm. Time-resolved data recorded on the millisecond time scale are shown in Figure S4 of the Supporting Information, and showed no further evolution. This contrasts with the work by Kraft et al. (9), who reported a small increase in the kinetics at 495 nm with a time constant of 5 ms. The main divergence between the steady-state absorption difference spectrum and that detected at 10 ns is due to a broad absorption at wavelengths longer than ~ 525 nm and an increased bleach below ~ 475 nm. To explore the kinetic behavior of the transient absorption signal, we measured time-resolved transients at two representative wavelengths: 495 nm, which corresponds to two characteristic peak in the absorption difference spectrum related to signaling-state

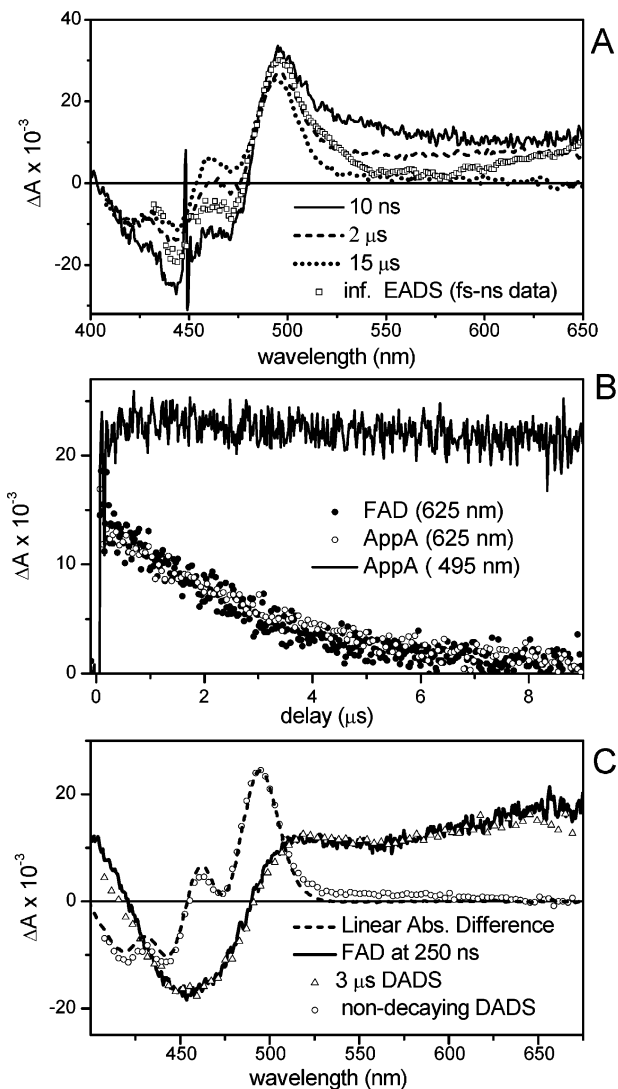


FIGURE 3: (A) Transient absorption difference spectra of AppA₅₋₁₂₅ at 10 ns (—), 2 μ s (---), and 15 μ s (···) and the nondecaying EADS obtained in the ultrafast data analysis (symbols) on excitation at 450 nm. (B) Time-resolved transient absorption kinetics of AppA₅₋₁₂₅ at 495 nm (—) and 625 nm (○). A transient absorption trace of pure FAD in the same buffer as AppA₁₋₁₂₅, measured at a wavelength of 625 nm, is shown as solid circles. (C) Decay-associated difference spectra (symbols) of AppA₅₋₁₂₅ obtained by global analysis of the microsecond transient absorption data, a transient absorption spectrum of pure FAD in the same buffer at a delay of 250 ns (—) and the steady-state absorption difference spectrum of the dark- and light-induced forms of AppA (---).

formation, and 625 nm, which corresponds to the induced absorption signal decaying fully within 15 μ s of excitation. These time-resolved traces are shown in Figure 3B by the solid line (495 nm) and empty symbols (625 nm). The absorption at 495 nm does not change significantly on time scales up to 10 μ s, while the signal at 625 nm fully decays monoexponentially with a time constant of ~ 3 μ s. Note that the signal at 495 nm shows some variation as a result from interference with the Q-switch from the Nd:YAG laser.

To determine the number of coexisting components in the nano- to microsecond transient absorption data, we performed a global kinetic analysis of the experimental data collected with the intensified CCD camera. The analysis included singular-value decomposition and global fitting as a sum of exponentials to extract the number of components, time

constants, and decay-associated difference spectra (DADS). Our analysis demonstrated that the data could well be fitted with two components: one exponential with a time constant of 3 μ s and one constant (nondecaying) component. The DADS obtained in the global fitting procedure are shown in Figure 3C by the circles (nondecaying component) and the triangles (3 μ s component). The nondecaying component has an absorption maximum at 495 nm and negative features at 442 and 420 nm. The dashed line in Figure 3C represents the steady-state absorption difference spectrum of light-induced and dark forms of AppA_{5–125}. The latter perfectly overlaps with one of the DADS extracted from the flash-photolysis data, indicating that this DADS is related to the signaling state of AppA_{5–125}. The shape of the second DADS (triangles) is similar to that observed for the flavin triplet state (17–20). To verify this assignment, we generated the triplet state in pure FAD dissolved in the same buffer as the protein by a pulsed nanosecond laser excitation at 450 nm. Note that under the conditions of the latter experiment practically no FAD semiquinone radical can be formed since no reducing agent is present in the sample. The FAD triplet difference spectrum (measured at the delay of 250 ns) is shown in Figure 3C as a solid line. It perfectly overlaps with the 3 μ s DADS of the protein sample. Moreover, the triplet state, generated in pure FAD, decays at a rate that corresponds exactly with the second component in AppA_{5–125}, as illustrated in Figure 3B (filled symbols). Thus, on the basis of our data, we conclude that the spectral component with a decay time of 3 μ s, observed in the protein sample, represents the FAD triplet state, which is formed in parallel with the signaling state, thereby presenting a side reaction that is not related to signaling-state formation. In this case, the DADS are also the species-associated difference spectra, since the parallel decays represent the correct physical picture.

The divergence between the 10 ns difference spectrum and the nondecaying EADS from the ultrafast data mainly concerns the extent of excited-state absorption around 540 nm. This can be ascribed to the presence of a small uncompensated contribution of stimulated emission in the latter spectrum, which arises from the small fraction of FAD chromophores with a nanosecond lifetime, which could not be well estimated in the global analysis procedure. Moreover, we noticed that the FAD triplet yield slightly varies from one AppA_{5–125} preparation to the other, leading to different amplitudes of the absorption in the region of 525–650 nm (results not shown). Note that the absorption maxima in the 10 ns spectrum (498 nm) and the nondecaying EADS of the ultrafast data (497 nm) are slightly red-shifted with respect to that recorded at 15 μ s (495 nm) because at these time delays, the red-shifted product state coexists with the triplet state: the triplet spectrum has a strongly varying absorption profile in this wavelength region, which leads to an apparent red shift of the product band to 497–498 nm.

Quantum Yield of Signaling-State Formation. Besides the time evolution of the photoreaction, the quantum yield of signaling-state formation is an important parameter for the biological function of the protein. To determine the quantum yield of the AppA^{dark state} \rightarrow AppA^{signaling state} phototransformation, we used a relative actinometric method with Ru(II)-trisbipyridine [Ru(bpy)₃²⁺] as a reference. The substantial overlap of the absorption spectra of AppA and Ru(bpy)₃²⁺ makes the latter compound a convenient reference substance

for determination of the phototransformation quantum yield. The quantum yield of the photoreaction (triplet-state formation) and the difference absorption coefficient of Ru(bpy)₃²⁺ have been established previously (21–24). The photoreaction was monitored by detection of transient absorption changes at wavelengths of 450 and 495 nm for Ru(bpy)₃²⁺ and AppA_{5–125}, respectively, after excitation at 450 nm (see also Figure S3 of the Supporting Information). The solutions of AppA_{5–125} and the reference substance were prepared with identical absorption at the excitation wavelength (see the inset in Figure S3 of the Supporting Information), which ensures that the same number of photons is absorbed by both samples. Series of measurements have been performed with different excitation energies to ensure linearity of the signal on the excitation energy at the light intensity that was used. To determine the quantum yield, absorbance changes of the solutions at the time of maximal concentration of the photoproduct state were assessed (see Figure S3 of the Supporting Information). The quantum yield of AppA_{5–125} signaling-state formation was determined using the following expression:

$$\Phi_{\text{AppA}} = \Phi_{\text{ref}} \frac{\Delta A_{\text{AppA}}^{(495)} \Delta \epsilon_{\text{ref}}^{(450)}}{\Delta A_{\text{ref}}^{(450)} \Delta \epsilon_{\text{AppA}}^{(495)}}$$

where Φ_{ref} is the quantum yield of the photoreaction of Ru(bpy)₃²⁺, $\Delta \epsilon_{\text{ref}}^{(450)}$ (M⁻¹ cm⁻¹) is the change in the absorption coefficient of Ru(bpy)₃²⁺ at 450 nm, $\Delta \epsilon_{\text{AppA}}^{(495)}$ (M⁻¹ cm⁻¹) is the change in the absorption coefficient of AppA_{5–125} at 495 nm, and ΔA is the absorbance change.

Using actual experimental parameters, the quantum yield of the AppA^{dark state} \rightarrow AppA^{signaling state} phototransformation is determined as follows:

$$\Phi_{\text{AppA}}^{\text{ref(Ru(bpy)}_3^{\text{2+}})} = 0.95(0.05) \times \frac{0.0051(0.0005) \times 7900(50)}{0.049(0.007) \times 3500(250)} = 0.24 \pm 0.07$$

Target Analysis, a Compartmental Model Approach. The time-resolved data on AppA_{5–125} shown in Figures 1–3 reveal the existence of multiple time scales of FAD* decay, the formation of a red-shifted intermediate which resembles the long-lived signaling state, and the formation of an additional product, presumably the FAD triplet state. However, from the data itself, it is not straightforward to extract the spectral and temporal information necessary to characterize the AppA photochemistry. To identify the various states in the AppA photocycle and analyze their dynamic behavior and connectivity, we globally analyzed the ultrafast time-resolved data with a target analysis. With a target analysis, the time-resolved data are described in terms of a kinetic scheme, which enables the estimation of the spectral signature and the lifetime of the “pure” molecular species that make up the spectral evolution of the system. The details of this method have recently been reviewed in ref 15. In particular, it is our goal to separate the contributions from the AppA red-shifted signaling state and the FAD triplet state in the spectral evolution. Moreover, we want to assess the contribution of each component of FAD* decay to the formation of the signaling state. On the basis of the knowledge obtained with the streak camera and ultrafast

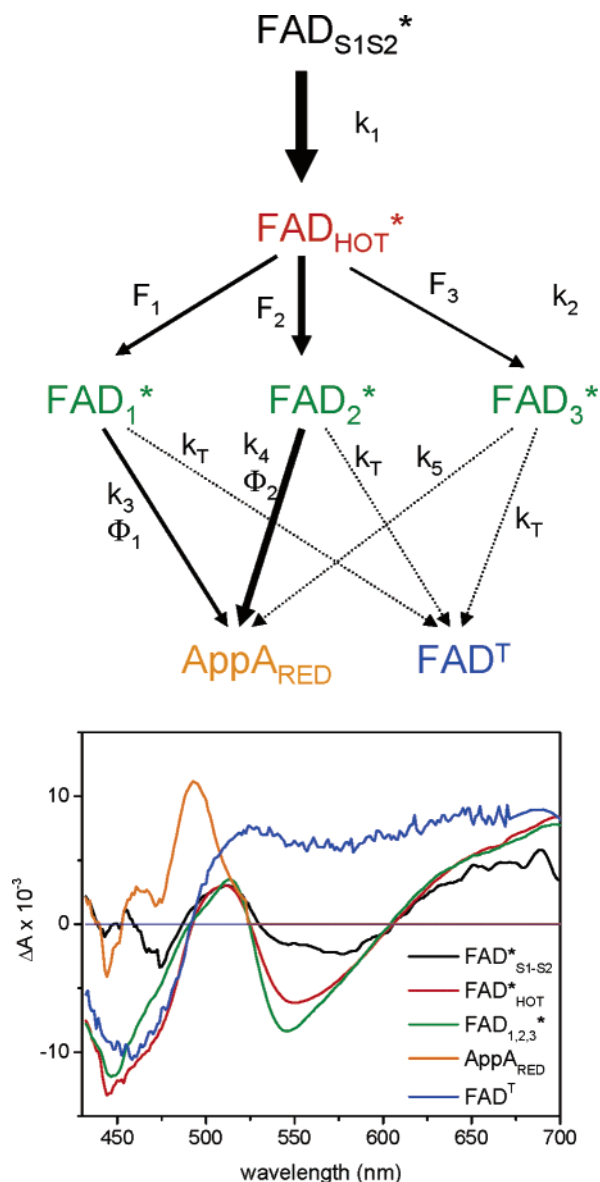


FIGURE 4: (Top) Kinetic scheme used to describe the spectral evolution of AppA_{5–125} by means of a target analysis. Here k_i is a rate constant; F_i denotes the fractional contribution of the FAD^{*} state, while Φ_i indicates the relative quantum yield of AppA_{RED}-state formation from the i th component. The width of the arrows roughly indicates the relative weight of the various reaction paths. (Bottom) Species-associated difference spectra (SADS) of the various molecular species in the kinetic scheme that result from the application of a target analysis to the ultrafast time-resolved data of AppA_{5–125}.

Table 1: Rate Constants, Fractional Contributions, and the Relative AppA_{RED}-State Yields that Result from Target Analysis of the Ultrafast Time-Resolved Data on AppA_{5–125} in Terms of the Kinetic Scheme Depicted in Figure 4

$k_1 = (170 \text{ fs})^{-1}$	$k_4 = (570 \text{ ps})^{-1}, F_2 = 0.59,$
$k_2 = (1.6 \text{ ps})^{-1}$	$\Phi_2 = 0.24$
$k_3 = (90 \text{ ps})^{-1}, F_1 = 0.38,$	$k_5 = (1000 \text{ ns})^{-1}, F_3 = 0.03$
$\Phi_1 = 0.23$	$k_T = (5 \text{ ns})^{-1}$

transient absorption experiments, we imposed a kinetic scheme as depicted in the top panel of Figure 4. The kinetic scheme encompasses the states identified in the sequential analysis of the ultrafast transient absorption data and the nanosecond flash-photolysis spectroscopic results: (1) the initially excited mixture of S₁ and S₂ states FAD^{*}_{S1–S2}, which

rapidly internally converts in ~ 250 fs to the “hot” FAD S₁ state, indicated in black; (2) the hot S₁ state FAD^{*}_{hot} which cools in ~ 1 ps, indicated in red; and (3) the relaxed singlet excited state of FAD, FAD^{*}, indicated in green. The heterogeneity in the relaxed FAD singlet excited-state decay can be assigned by assuming three compartments with different decay times, denoted FAD₁^{*}, FAD₂^{*}, and FAD₃^{*}. This assumption is equivalent to the adoption of a physical model in which the multiexponentiality arises from a heterogeneity that exists in the ground state of AppA. (4) The red-shifted product state absorbing near 495 nm, indicated in orange. In the absence of an established nomenclature, we have provisionally denoted this state as “AppA_{RED}”. (5) The FAD triplet state, FAD^T, indicated in blue. In the kinetic model, the three FAD^{*} compartments are allowed to evolve into the AppA_{RED} product, but only the first two, which represent the FAD^{*} decay on the 90 and 590 ps time scales, have a significant contribution in the light of their amplitudes. The third compartment represents the small fraction of FAD^{*} that has a nanosecond lifetime. The rate of intersystem crossing to the triplet state in flavins has been estimated to lie between $(8 \text{ ns})^{-1}$ in aqueous solution and $\sim (3 \text{ ns})^{-1}$ in LOV photoreceptors (17, 25). Accordingly, an intersystem crossing rate of $(5 \text{ ns})^{-1}$ to FAD^T is fixed in the FAD₁^{*}–FAD₃^{*} decay compartments, where it competes with AppA_{RED} product-state formation. This implies that a small yield of FAD triplets will always be formed in AppA irrespective of the reaction model, simply on the basis of the dominant FAD^{*} lifetime of ~ 590 ps.

In accordance with the quantum yield experiments presented above, a yield of 24% is fixed in the evolution of the dominant FAD₂^{*} compartment into the AppA_{RED} compartment, whereby the remaining 76% of the population of this state either evolved into the triplet state or was deactivated to the FAD ground state. The AppA_{RED} yield from the FAD₁^{*} compartment was a free parameter. The SADS of FAD^T is taken from the nanosecond flash-photolysis results of Figure 3 and fixed in the target analysis procedure. The SADS associated with FAD₁^{*}–FAD₃^{*} were required to be identical for all three compartments, which is reasonable given the virtual absence of spectral evolution in the fluorescence streak camera experiments (see Figure 1). The SADS of the AppA_{RED} species is assumed to be zero at wavelengths beyond 520 nm. This leaves as free parameters the SADS of FAD₁^{*}–FAD₃^{*} and AppA_{RED}, rates k_1 – k_5 , fractions of FAD^{*} decay F_1 – F_3 , the AppA_{RED} yield from FAD₁^{*} (Φ_1) and the parameters describing pulse width, time zero, and the group velocity dispersion in the white light continuum.

The SADS that result from the target analysis are shown in the bottom panel of Figure 5, whereas the fitted rate constants, FAD decay fractions, and fractional contributions to AppA_{RED} formation are listed in Table 1. As expected, the SADS of FAD^{*}_{S1–S2}, FAD^{*}_{hot}, and FAD^{*} are practically identical to the first three components in the sequential analysis procedure of Figure 2D. Moreover, the fitted FAD^{*} internal conversion (170 fs), vibrational cooling (1.6 ps), and decay times (90 ps, 570 ps, and 5 ns) correspond well with the result from the sequential analysis (250 fs, 1.2 ps, 90 ps, 590 ps, and 2.7 ns). Note that these times need not be exactly identical. The SADS of AppA_{RED} and FAD^T are nicely separated, and reveal a spectral shape of AppA_{RED} very similar to that of the long-lived red-shifted intermediate in

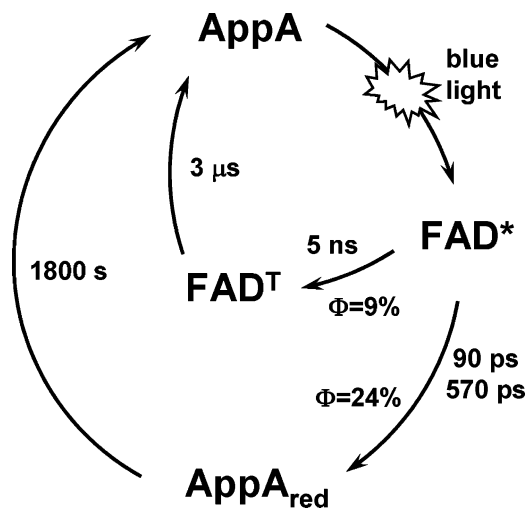


FIGURE 5: Photocycle scheme of AppA₅₋₁₂₅.

the AppA photocycle and that extracted from the nanosecond flash-photolysis experiments, with a prominent absorption band at 494 nm, and a pattern of minor bands at 471 nm (minimum), 463 nm (maximum), and 443 nm (minimum). Importantly, the relative yield of AppA_{RED} formation from the FAD₁* compartment was estimated to be ~20%, comparable to that of the dominant FAD₂* compartment.

Several conclusions are drawn from the target analysis. Most importantly, the AppA_{RED} state, which strongly resembles the long-lived signaling state, is directly formed from the FAD singlet excited state without any apparent intermediate. This occurs with time constants of 90 and 570 ps, of which the latter forms the dominant contribution. The AppA_{RED} yield from each of the components is similar and, in keeping with the quantum yield experiments presented in the previous section, is estimated to be 20–24%. The formation of the FAD^T state arises mainly from the longer-lived components in the FAD* decay: FAD₂* contributes a total triplet yield of 6%, whereas FAD₃* contributes 3%, giving a total triplet yield of 9%.

DISCUSSION

The application of time-resolved spectroscopy from the femtosecond to microsecond time scale has allowed a complete characterization of the AppA₅₋₁₂₅ photocycle to the extent allowed by the methods of optical spectroscopy. The photocycle is summarized in the scheme depicted in Figure 5. The time-resolved fluorescence experiments have shown that the decay of excited AppA-bound FAD is highly multiexponential. Ultrafast transient absorption experiments demonstrate that concomitant with the decay of excited FAD in 90 and 570 ps, a red-shifted intermediate state provisionally labeled AppA_{RED} is formed that strongly resembles the long-lived signaling state of AppA₅₋₁₂₅. Consistent with these results, the nanosecond flash-photolysis experiments have shown that within the time resolution of 10 ns, formation of the AppA₅₋₁₂₅ signaling state is complete. It is generated with a quantum yield of 24% and remains unaltered up to the microsecond time scale. In parallel with formation of the AppA_{RED} state, FAD triplet states are formed at a low yield of ~9%. The nanosecond flash-photolysis experiments have shown that these FAD triplets represent a side reaction and are not coupled to the physiologically relevant reaction

pathway. These triplet states decay to the molecular ground state in 3 μ s. This is in contrast with the photoactivation mechanism of the flavin binding LOV domains, where the triplet state of the flavin is involved in signaling-state formation based on the formation of a covalent adduct between the chromophore and a conserved cysteine (17, 19, 20). The AppA signaling state thermally recovers to the dark state in 1800 s (9, 10).

AppA₅₋₁₂₅ has a unique photocycle compared to other photoreceptors such as PYP, LOV domains, or the rhodopsins. In these photoreceptors, multiple spectroscopically distinguishable photocycle intermediates follow one another on increasing time scales, thereby altering the physicochemical state of the chromophore and gradually decreasing the free energy of the system until a stable, long-lived signaling state is reached (26). Here we have shown that in AppA₅₋₁₂₅, there is just one clearly distinct photocycle intermediate, generated directly from the FAD singlet excited state. After this intermediate state is formed on ultrafast time scales of 90 and 570 ps, no spectroscopically distinguishable changes over 12 decades of time can be detected with UV–visible spectroscopy. This presents a paradox: on one hand, formation of the signaling state in AppA₅₋₁₂₅ is faster than in any other photoreceptor, while on the other hand, with a lifetime of 1800 s the AppA₅₋₁₂₅ signaling state ranks among the most thermally stable. This raises fundamental questions about the way in which the AppA signaling state is energetically stabilized and how fast back-reactions to the dark state are prevented.

No photochemical reaction mechanism can be proposed on the basis of these experiments. The optical measurements did not provide sufficient information allowing for a more detailed interpretation of the precise molecular events that underlie the AppA photochemistry. However, given the ultrafast time scales, the changes that lead to the red-shifted product must be very local and confined to the immediate environment around the chromophore. The absence of absorbance changes in the UV–visible region from the 10⁻⁹ to 10³ second time scales does not necessarily imply that no functional structural changes of AppA₅₋₁₂₅ occur in this time window. The structural changes of the AppA₅₋₁₂₅ protein backbone may be silent with respect to perception by the chromophore. Such well-studied photoreceptor proteins, such as rhodopsins and photoactive yellow protein (1), demonstrate that the global changes in the protein structure in response to the chromophore photoactivation take place on the microsecond to millisecond time scales. However, the absence of the significant dynamics in the spectral response of the chromophore of AppA₅₋₁₂₅ may also be explained by relatively minor photoinduced structural transformations of the protein construct used in these studies. To reveal the structural dynamics of this protein, further studies, for example, time-resolved infrared spectroscopy and transient grating and pulsed laser-induced photoacoustic spectroscopy (27), need to be carried out. However, we can safely state that the physicochemical state of the FAD cofactor remains largely unaltered over this vast time range.

We have estimated a quantum yield of 24% for signaling-state formation of 24% and a FAD^T yield of 9% in AppA₅₋₁₂₅. This implies that during the excited-state lifetime, ca. 67% of FAD* is deactivated to the ground state. The natural lifetime of singlet-excited flavin is determined by intersystem crossing, radiative decay, and internal conversion, and is on

the order of 5 ns (16, 17), 1 order of magnitude longer than the FAD* lifetime in AppA. This implies that another radiationless deactivation mechanism must be active in AppA₅₋₁₂₅ which competes with AppA_{RED} formation. It was shown that in flavoenzymes, efficient electron and proton transfer may occur from aromatic residues to the flavin, after which the radical pair rapidly recombines on the picosecond time scale to the flavin ground state (28). AppA₅₋₁₂₅ contains several aromatic amino acids which could similarly deactivate the singlet excited state of FAD. From our ultrafast data, there is no evidence for such processes; however, they could escape detection if the recombination rate would be higher than that of the initial electron transfer event.

We have shown that the excited-state decay of AppA₅₋₁₂₅ is highly multiexponential, as indicated by time-resolved fluorescence and ultrafast transient absorption experiments. The origin for this multiexponentiality is thus far unclear: we have modeled our ultrafast time-resolved data assuming that it results from heterogeneity in the ground-state conformation of AppA₅₋₁₂₅, leading to a “fast”, a “medium”, and a “slow” reacting fraction. Alternative physical models can account for the observed multiexponential decay as well: a reaction mechanism can be imagined assuming the establishment of a dynamic equilibrium between FAD* and AppA_{RED}, with the AppA_{RED} state subsequently relaxing to a lower free energy on the (sub)nanosecond time scale. Such models have, for instance, been invoked to explain the multiexponential decay of chlorophyll excited states in photosynthetic reaction centers (29).

ACKNOWLEDGMENT

We thank Elena Andrizhiyevskaya for useful advice on the streak camera setup and Mattijs de Groot for his assistance in nanosecond transient absorption measurements.

SUPPORTING INFORMATION AVAILABLE

Time-resolved fluorescence and absorption data on AppA₅₋₁₂₅ represented by the DAS and EADS of Figures S1 and S2, respectively; the AppA₅₋₁₂₅ quantum yield experiment; and AppA₅₋₁₂₅ dynamics on the millisecond time scale. This material is available free of charge via the Internet at <http://pubs.acs.org>.

REFERENCES

- van der Horst, M. A., and Hellingwerf, K. J. (2004) Photoreceptor Proteins, “Star Actors of Modern Times”: A Review of the Functional Dynamics in the Structure of Representative Members of Six Different Photoreceptor Families, *Acc. Chem. Res.* **37**, 13–20.
- Fankhauser, C., and Chory, J. (1999) Photomorphogenesis: Light receptor kinases in plants! *Curr. Biol.* **9**, R123–R126.
- Briggs, W. R., and Huala, E. (1999) Blue-light photoreceptors in higher plants, *Annu. Rev. Cell Dev. Biol.* **15**, 33–62.
- Braatsch, S., and Klug, G. (2004) Blue light perception in bacteria, *Photosynth. Res.* **79**, 45–57.
- Salomon, M., Christie, J. M., Knieb, E., Lempert, U., and Briggs, W. R. (2000) Photochemical and mutational analysis of the FMN-binding domains of the plant blue light receptor, phototropin, *Biochemistry* **39**, 9401–9410.
- Gomelsky, M., and Klug, G. (2002) BLUF: A novel FAD-binding domain involved in sensory transduction in microorganisms, *Trends Biochem. Sci.* **27**, 497–500.
- Gomelsky, M., and Kaplan, S. (1998) AppA, a Redox Regulator of Photosystem Formation in *Rhodobacter sphaeroides* 2.4.1, Is a Flavoprotein, *J. Biol. Chem.* **273**, 35319–35325.
- Masuda, S., and Bauer, C. E. (2002) AppA Is a Blue Light Photoreceptor that Antirepresses Photosynthesis Gene Expression in *Rhodobacter sphaeroides*, *Cell* **110**, 613–623.
- Kraft, B. J., Masuda, S., Kikuchi, J., Dragnea, V., Tollin, G., Zaleski, J. M., and Bauer, C. E. (2003) Spectroscopic and mutational analysis of the blue-light photoreceptor AppA: A novel photocycle involving flavin stacking with an aromatic amino acid, *Biochemistry* **42**, 6726–6734.
- Laan, W., van der Horst, M. A., van Stokkum, I. H., and Hellingwerf, K. J. (2003) Initial characterization of the primary photochemistry of AppA, a blue-light-using flavin adenine dinucleotide-domain containing transcriptional antirepressor protein from *Rhodobacter sphaeroides*: A key role for reversible intramolecular proton transfer from the flavin adenine dinucleotide chromophore to a conserved tyrosine? *Photochem. Photobiol.* **78**, 290–297.
- Masuda, S., Hasegawa, K., Ishii, A., and Ono, T. (2004) Light-induced structural changes in a putative blue-light receptor with a novel FAD binding fold sensor of blue-light using FAD (BLUF); Slr1694 of *Synechocystis* sp. PCC6803, *Biochemistry* **43**, 5304–5313.
- Laan, W., Bednarz, T., Heberle, J., and Hellingwerf, K. J. (2004) Chromophore composition of a heterologously expressed BLUF-domain, *Photochem. Photobiol. Sci.* **3**, 1011–1016.
- Gobets, B., van Stokkum, I. H. M., Rogner, M., Kruip, J., Schlodder, E., Karapetyan, N. V., Dekker, J. P., and van Grondelle, R. (2001) Time-Resolved Fluorescence Emission Measurements of Photosystem I Particles of Various Cyanobacteria: A Unified Compartmental Model, *Biophys. J.* **81**, 407–424.
- Gradinaru, C. C., Kennis, J. T. M., Papagiannakis, E., van Stokkum, I. H. M., Cogdell, R. J., Fleming, G. R., Niederman, R. A., and van Grondelle, R. (2001) An unusual pathway of excitation energy deactivation in carotenoids: Singlet-to-triplet conversion on an ultrafast time scale in a photosynthetic antenna, *Proc. Natl. Acad. Sci. U.S.A.* **98**, 2364–2369.
- van Stokkum, I. H. M., Larsen, D. S., and van Grondelle, R. (2004) Global and target analysis of time-resolved spectra, *Biochim. Biophys. Acta* **1657**, 82–104.
- Van den Berg, P. A. W., and Visser, A. J. W. G. (2001) *New Trends in Fluorescence Spectroscopy: Applications to Chemical and Life Sciences* (Valeur, B., and Brochon, J.-C., Eds.) p 457, Springer, Berlin.
- Kennis, J. T. M., Crosson, S., Gauden, M., van Stokkum, I. H. M., Moffat, K., and van Grondelle, R. (2003) Primary reactions of the LOV2 domain of phototropin, a plant blue-light photoreceptor, *Biochemistry* **42**, 3385–3392.
- Sakai, M., and Takahashi, H. (1996) One-electron photoreduction of flavin mononucleotide: Time-resolved resonance Raman and absorption study, *J. Mol. Struct.* **379**, 9–18.
- Swartz, T. E., Corchnoy, S. B., Christie, J. M., Lewis, J. W., Szundi, I., Briggs, W. R., and Bogomolni, R. A. (2001) The photocycle of a flavin-binding domain of the blue light photoreceptor phototropin, *J. Biol. Chem.* **276**, 36493–36500.
- Kottke, T., Heberle, J., Hehn, D., Dick, B., and Hegemann, P. (2003) Phot-LOV1: Photocycle of a blue-light receptor domain from the green alga *Chlamydomonas reinhardtii*, *Biophys. J.* **84**, 1192–1201.
- Creutz, C., Chou, M., Netzel, T. L., Okumura, M., and Sutin, N. (1980) Lifetimes, spectra, and quenching of the excited states of polypyridine complexes of iron(II), ruthenium(II), and osmium(II), *J. Am. Chem. Soc.* **102**, 1309–1319.
- Crosby, G. A., and Demas, J. N. (1971) Quantum efficiencies on transition metal complexes. II. Charge-transfer luminescence, *J. Am. Chem. Soc.* **93**, 2841.
- Bensasson, R., Salet, C., and Balzani, V. (1976) Laser flash spectroscopy of tris(2,2'-bipyridine)ruthenium(II) in solution, *J. Am. Chem. Soc.* **98**, 3722–3724.
- Bensasson, R., Salet, C., and Balzani, V. (1979) Spectre d'absorption et rendement quantique de formation du premier état excité triplet du ruthenium (II) tris(2,2'-bipyridine) en solution aqueuse, *C. R. Hebd. Seances Acad. Sci., Ser. B* **289**, 41–43.
- Holzer, W., Penzkofer, A., Fuhrmann, M., and Hegemann, P. (2002) Spectroscopic characterization of flavin mononucleotide bound to the LOV1 domain of Phot1 from *Chlamydomonas reinhardtii*, *Photochem. Photobiol.* **75**, 479–487.
- Losi, A., and Braslavsky, S. E. (2003) The time-resolved thermodynamics of the chromophore-protein interactions in biological photosensors as derived from photothermal measurements, *Phys. Chem. Chem. Phys.* **5**, 2739–2750.

27. Takeshita, K., Imamoto, Y., Kataoka, M., Mihara, K., Tokunaga, F., and Terazima, M. (2002) Structural change of site-directed mutants of PYP: New dynamics during pR state, *Biophys. J.* 83, 1567–1577.
28. Zhong, D. P., and Zewail, A. H. (2001) Femtosecond dynamics of flavoproteins: Charge separation and recombination in riboflavin (vitamin B-2)-binding protein and in glucose oxidase enzyme, *Proc. Natl. Acad. Sci. U.S.A.* 98, 11867–11872.
29. Muller, M. G., Hucke, M., Reus, M., and Holzwarth, A. R. (1996) Primary processes and structure of the photosystem II reaction center. 4. Low-intensity femtosecond transient absorption spectra of D1-D2-cyt-b559 reaction center, *J. Phys. Chem.* 100, 9527–9536.

BI047359A